Supporting Information

Remarkable sol-gel transition of PNIPAm-based nanogels *via* large steric hindrance of side-chain

*Xiaoxiao Li [a,d] ‖, Xueting Li[a,b,c] ‖, Tingting Xia[a], Wei Chen[a], Kenneth J. Shea[e] and Xihua Lu [a,b,c]**

[a] *College of Chemistry and Chemical Engineering, Donghua University, Shanghai 201620, People's Republic of China.*

[b] *Fujian Nano-Micro Advanced Materials Sci. & Tech. Co. Ltd., Three Creation Park, Jinjiang, Fujian 362200, People's Republic of China.*

[c] *Anhui Microdelivery Smart Microcapsule Sci. & Tech. Co. Ltd., Tongling, Anhui 244000, People's Republic of China.*

[d] *Department of Orthopaedics, Shanghai Key Laboratory for Prevention and Treatment of Bone and Joint Diseases, Shanghai Institute of Traumatology and Orthopaedics, Ruijin Hospital, Shanghai Jiao Tong University School of Medicine, Shanghai, 200025, People's Republic of*

[e] *Department of Chemistry, University of California, Irvine, California 92697, United States.*

‖ These authors contributed equally to this work.

E-mail: luxihua@dhu.edu.cn, Fax: +86216779 2776; Tel: +86 216779 2776

Experimental Section

Methods

Materials. *N*-Isopropylacrylamide (NIPAm, 97%, Aldrich), *N*-tert-butylacrylamide (TBA, 99%, Aldrich), *N*, *N*'-methylenebisacrylamide (BIS, 99%, Aldrich), Ammonium persulfate (APS, 98%, Aldrich), Sodium dodecyl sulfate (SDS, 99%, Aldrich), *L*-phenyl alanine (99%, Aldrich), Acryloylchloride (99%, Aldrich). All chemicals were used without further purification.

Synthesis of PNIPAm and PNT nanogels. The PNT nanogels (PNT NPs) were synthesized by emulsion precipitation polymerization. Briefly, all the co-monomers (NIPAm, TBA, BIS) and surfactant SDS (0.04 g, 0.15 mmol) were dissolved in water (80 mL). The total monomer in feed was 10 mmol, while the molar ratio of the co-monomers, (98-x/x/2) (NIPAm/TBA/BIS), was varied according to the desired TBA content. The reaction mixture was heated to 70 °C under nitrogen. After 30 min, APS (0.06 g, dissolved in 5 mL of ultrapure water) was added to initiate the reaction. The reaction was proceeded for 4 h. The resulting nanogels were denoted as PNIPAm, PNT12, PNT16, PNT22, PNT28 and PNT36, according to the TBA content, which

was 0, 12, 16, 22, 28 and 36 mol%, respectively. The obtained NPs were purified by dialysis (MWCO=8000-14000 Da) against ultrapure water for one week.

Synthesis of APhe monomer. Briefly, *L*-phenyl alanine (7.2 g, 43 mmol) was dissolved in 40 mL of 2 M sodium hydroxide aqueous solution at 0 ^{o}C. Acryloylchloride (3.7 mL, 46 mmol) was added to the solution dropwise and stirred at 0 ^{o}C for 2 h. The solution was acidified by 5 N HCl (PH < 2) and a precipitated white solid was filtered and dried (yield: 43%).

^{1}H NMR (600 MHz, $CDCl_3$, **Figure S10**): δ (ppm) =12.77 (1H, s), 8.44 (2H, d), 7.19-7.26 (5H, m), 6.07 (1H, dd), 6.04 (1H, dd), 5.60 (1H, dd), 4.49 (1H, m), 3.09 (1H, q), 2.91 (1H, q)

Synthesis of PNTA nanogels. The synthesis of PNTA nanogels (PNTA NPs) was by using the same method as that of PNT NPs, while the molar ratio of the co-monomers was (82/12/4/2) (NIPAm/TBA/Aphe/BIS). The resultant nanogels, denoted as PNTA NPs, were purified by dialysis (MWCO=8000-14000 Da) against ultrapure water for one week.

Characterizations. The particle sizes of prepared NPs ($1.0*10^{-5}$ g/ mL) were measured by dynamic light scattering (DLS) with a BI-9000 AT digital time correlator (BI-200SM, Brookhaven Instruments, Inc.) at various temperatures and a scattering angle of 90^{o}. Modulated temperature DSC traces were analyzed with a TA Instruments D2500 with an RCS refrigeration control system under nitrogen flow. Scans were run with a scanning rate at 5 ^{o}C/min. The reflection spectra of the PNTA colloidal crystals were measured by an Ocean Optics PG2000-Pro-EX spectrometer. Transmission electron microscopy (TEM, Talos F200X G2, US) was used to observe the morphology of PNT12 nanogel.

Rheological Measurements. Dynamic rheological analysis was carried out in a stain-controlled ARES rheometer. The parallel plate geometry with the plate diameter of 60 mm was used, and the sample gap was adjusted to 1 mm. Temperature-dependent changes in storage modulus, G', and loss modulus, G'', were recorded in a dynamic temperature ramp test with a heating rate of 2 ^{o}C/min. The temperature was controlled by a peltier system in the bottom plate connected with a water bath. The rheological experiments were performed within the linear viscoelastic region (strain 1%, angular frequency 6.28 rad/s).

Temperature-variable FTIR spectroscopy. PNT12 NPs and PNIPAm NPs powder was respectively swollen in D_2O (6 wt%) at 4 ^{o}C for one week to ensure complete deuteration of all the N-H protons and sufficient swelling. A drop of the swollen NPs dispersion was being sealed between two calcium fluoride (CaF_2) tablets. All time-resolved FTIR spectra at different

temperatures were recorded on a Nicolet Nexus 670 spectrometer with a resolution of 4 cm^{-1} and 16 scans. Spectra were collected over the temperature range with manually controlled heating rate of 1 °C/min.

Temperature-variable ^{1}H NMR. ^{1}H NMR spectra of PNT12 and PNIPAm NPs in D_2O were measured by using a Bruker Avance III spectrometer operating at 600 MHz for protons equipped with a temperature control unit. The integrated intensities were determined by the software of MestreNova at an accuracy of ±1%.

To quantitatively characterize the phase separation, we plotted the temperature dependences of the phase separation fraction ρ for different proton types in PNTA NPs, PNT12 NPs and PNIPAm NPs, where ρ is defined as

$$\rho = 1 - I/I_0 \quad (1)$$

I and I_0 were the normalized integrated intensities of a selected resonant peak at a specified temperature and the initial temperature. The normalization was performed according to the integrated intensity of HDO peak from the solvent. While the HDO peak did not shift over the whole temperature range.

Sol-gel transition. The sol-gel transition of the concentrated NPs dispersion was examined by using a vial tilting method as a function of temperature. The concentrated NPs dispersions with various concentrations were prepared in a glass vial, and kept at 4 °C prior to the experiment. The experiment was carried out in an incubator from 10 °C to 40 °C at 1 °C intervals, and at each temperature the samples were equilibrated for 5 min before visual observation. The gel phase was determined by tilting the vial when no fluidity was visually observed after 1 min.

Shrinking Kinetics above phase transition temperature. The shrinking kinetics of in-situ forming hydrogel were measured gravimetrically at different temperature. At predetermined time intervals, the supernatant was taken out and weighed. Water retention was defined as follows:

$$\text{Water retention \%} = \left(1 - \frac{Wt}{W0}\right)*100 \quad (2)$$

Where W_t was the weight of the supernatant at time t, W_0 was the initial weight of water in PNT NPs.

Cell culture. Helf cells were cultured in DMEM (Hyclone, USA) culture media containing 10% fetal bovine serum, 50 units/mL penicillin and 50 units/mL streptomycin at 37 ℃, 5% CO_2/95% air (v/v) environment.

Cell viability. Cell viability was measured by MTT assay. Helf cells were seeded in 96-well plates at a density of 8×10^3 cells per well and cultured for overnight. Different formulations were added with predetermined nanogel concentrations and incubated for another 24 h. Thereafter, 20 µl of 3-[4, 5-dimethylthiazol-2-yl]-3, 5 diphenyltetrazolium bromide solution (MTT, 5 mg/mL in PBS solution) was added to each well. After incubating for another 4 h at 37 ^oC, the media was removed and 150 µl of DMSO was added to dissolve formazan crystal. The cells were visualized under a laser scanning confocal microscope (Leica TCS SP8 STED 3X).

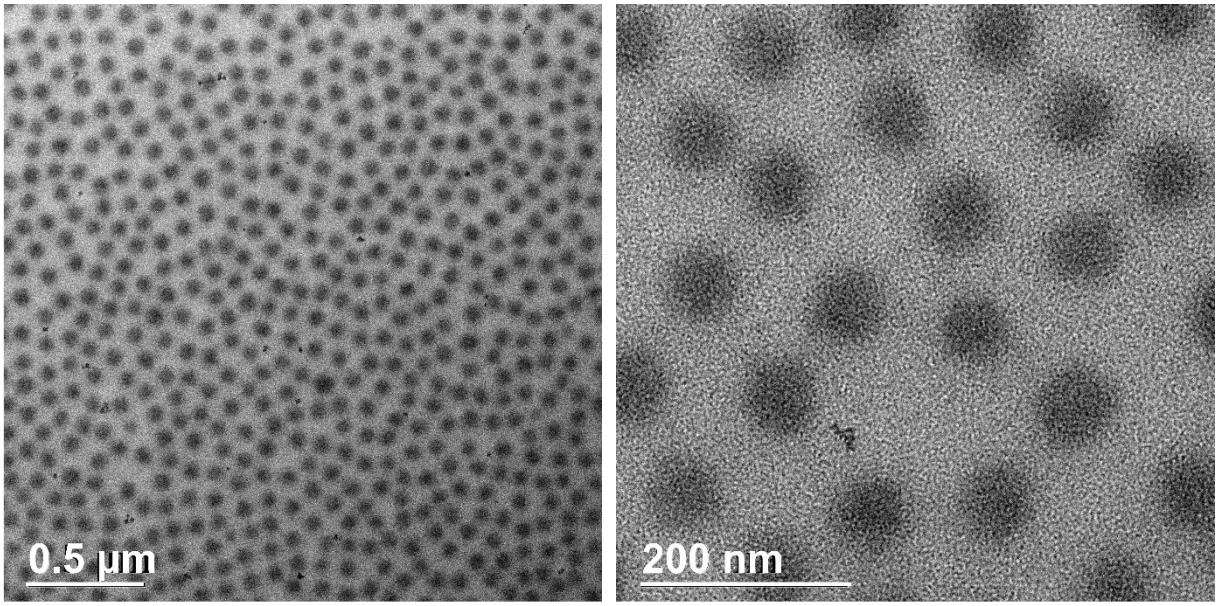

Figure S1. TEM images of PNT12 NPs in different scale bars.

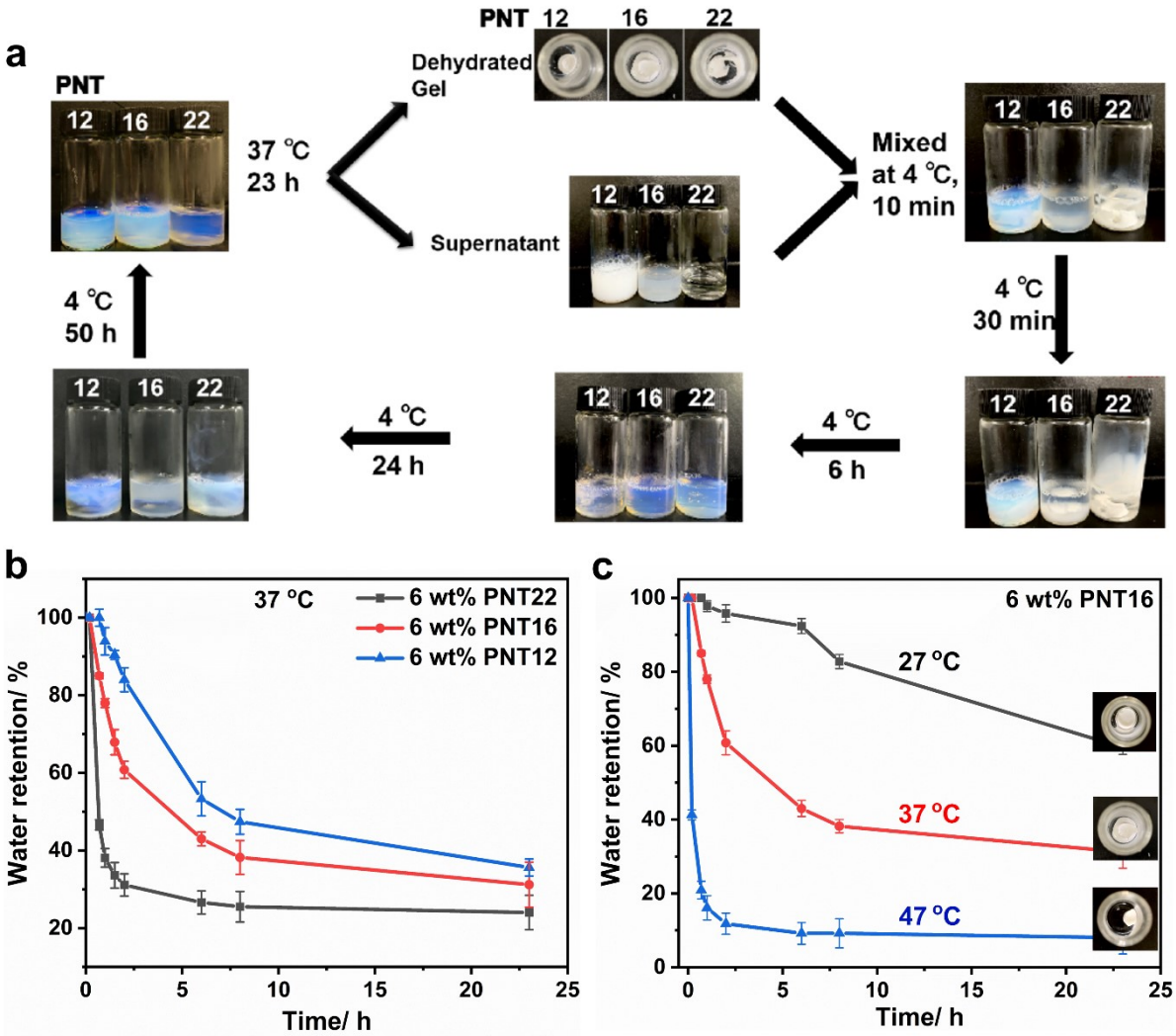

Figure S2. (a) Schematic diagram of deswelling/swelling process for PNT NPs (6 wt%). (b) Water retention for PNT NPs against the incubation time at 37 °C. (c) Water retention for PNT16 NPs (6 wt%) against the incubation time at different temperature.

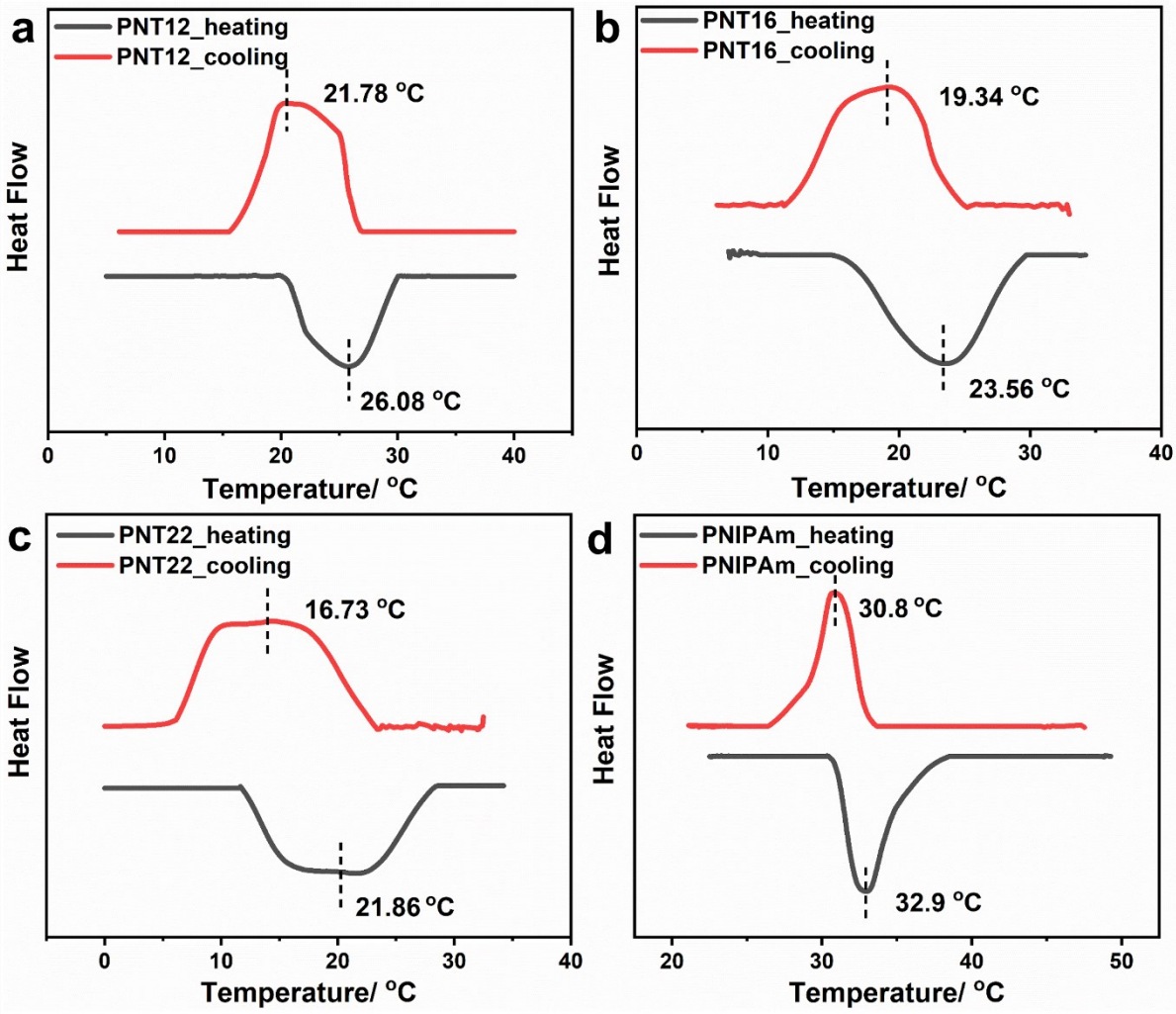

Figure S3. DSC curves for (a) PNT12 NPs, (b) PNT16 NPs, (c) PNT22 NPs, and (d) PNIPAm NPs during heating/cooling process. The testing concentration of all NPs was 6 wt%.

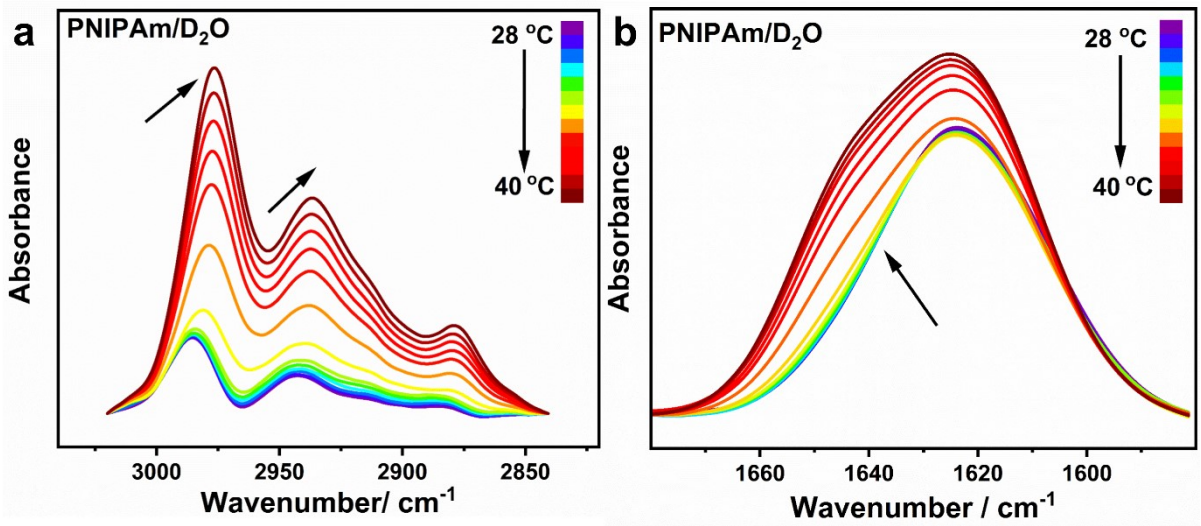

Figure S4. Temperature-dependent FTIR spectra of PNIPAm NPs (D_2O) during heating between 28 and 40 °C with interval of 1 °C. (a) The C-H regions, (b) The C=O regions (Normalized curves).

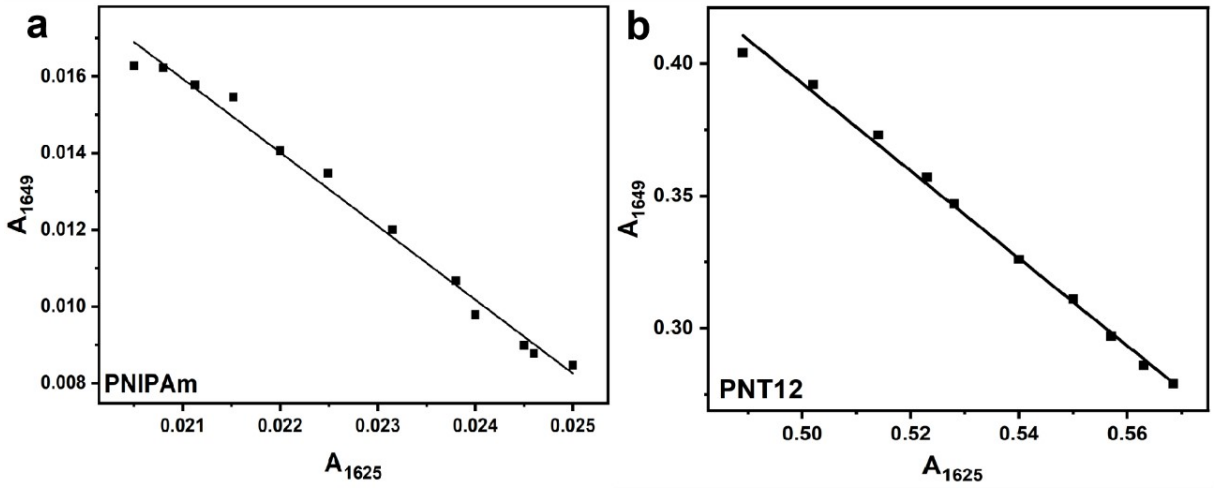

Figure S5. (a) Relative areas of 1649 cm^{-1} of the C=O···D-N hydrogen bond in PNIPAm D_2O dispersion (6 wt%), and (b) in PNT12 D_2O dispersion (6 wt%) at different temperatures were plotted against the intensity of the 1625 cm^{-1} component (C=O···D-O-D hydrogen bond). The slope of the fitting line yields the ratio of the molar absorption coefficient ($\varepsilon_{1649}/\varepsilon_{1625}$) was 1.92 and 0.98 respectively.

Presuming a 1:1 conversion of the carbonyls (C=O···D-O-D and C=O···D-N), the f(C=O···D-N) was calculated by means of curve fitting (**Figure 3e-f**). When the peak intensity of one component is plotted as a function of the other component, the slope of the fitted line, yields the ratio of the molar absorptivity of C=O···D-N relative to that of C=O···D-O-D, as shown in **Figure S5 (a)-(b)**.

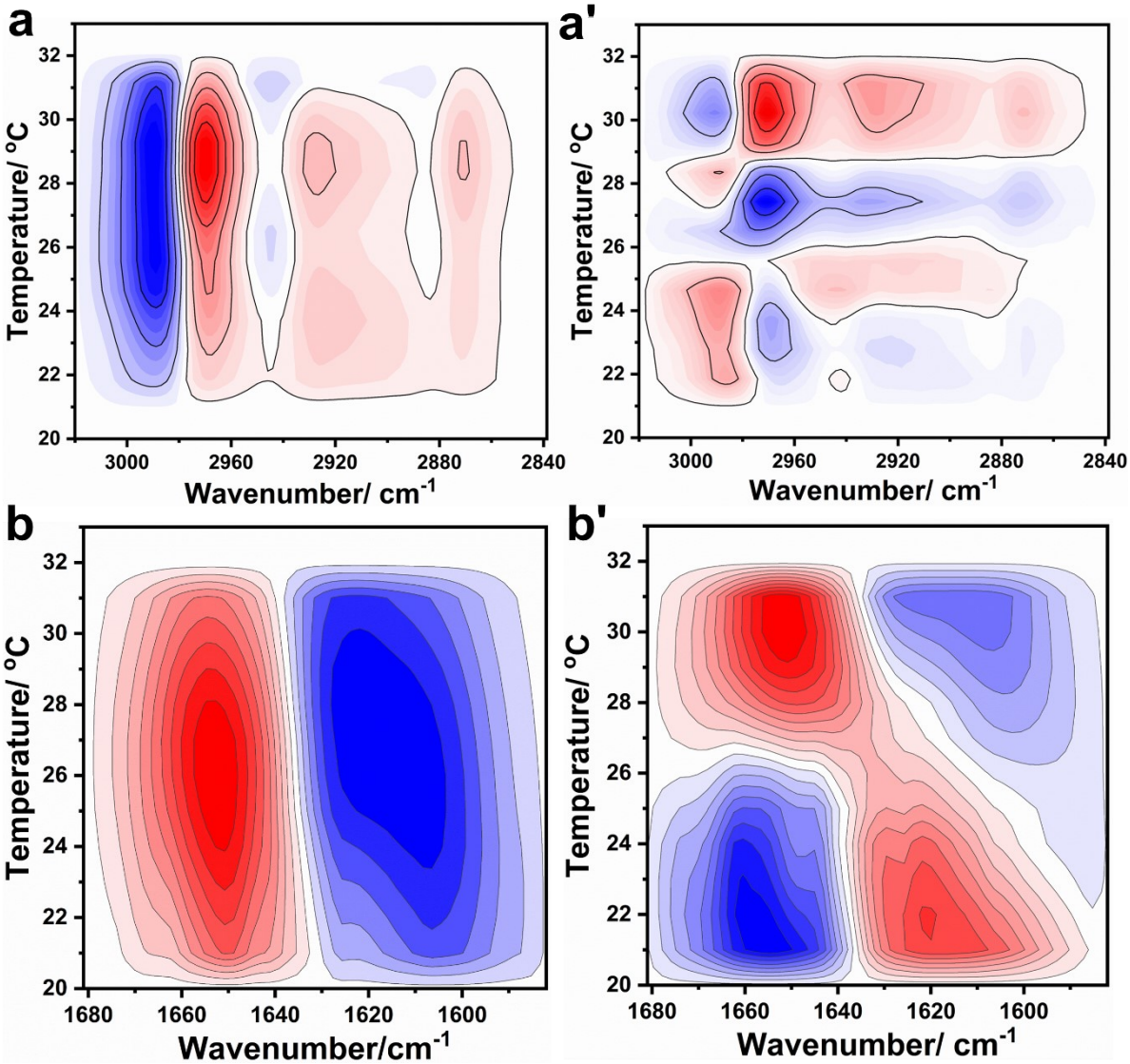

Figure S6. 2D synchronous (a), (b) and asynchronous (a') and (b') spectra of PCMW performed from 20 to 33 °C in the C-H regions (a, a') and the C=O regions (b, b') of PNT12 NPs.

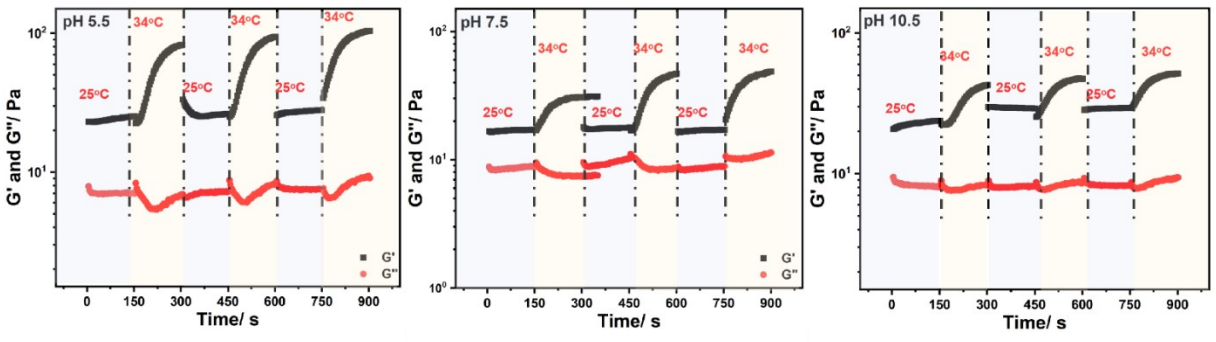

Figure S7. Thermo-reversibility and stability of PNTA NPs (3 wt%) at 25 °C and 34 °C at different pH values.

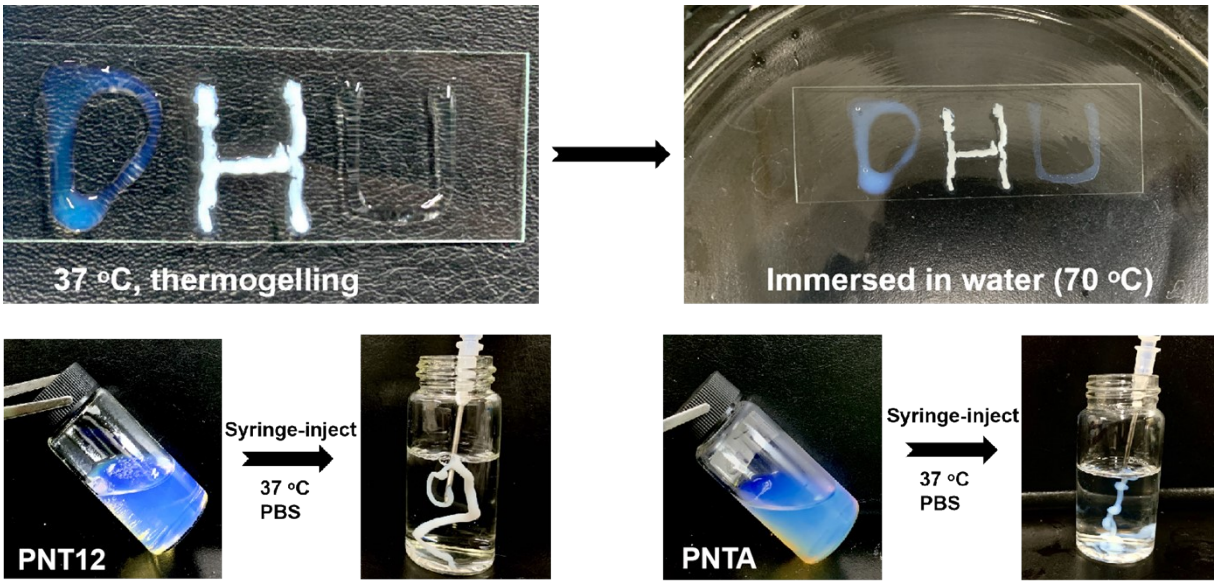

Figure. S8 Photographs of PNT12 NPs and PNTA NPs after thermogelling at 37 °C (left) and immersing in hot water (right). Character D: PNTA NPs (3 wt%) at pH 5.5; Character H: PNT12 NPs (6 wt%); Character U: PNTA NPs (3 wt%) at pH 10.5 (b) Syringe-injectable property of PNT12 (6 wt%) and PNTA NPs (3 wt%).

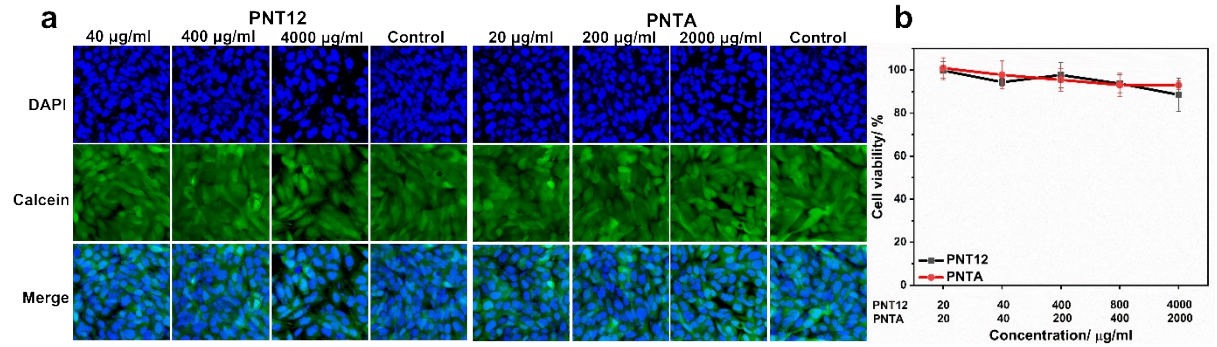

Figure. S9 (a) Fluorescence images of live stain for PNT12 NPs and PNTA NPs at 24 h. (b) Cell viability of PNT12 NPs and PNTA NPs via MTT assay at 24 h.

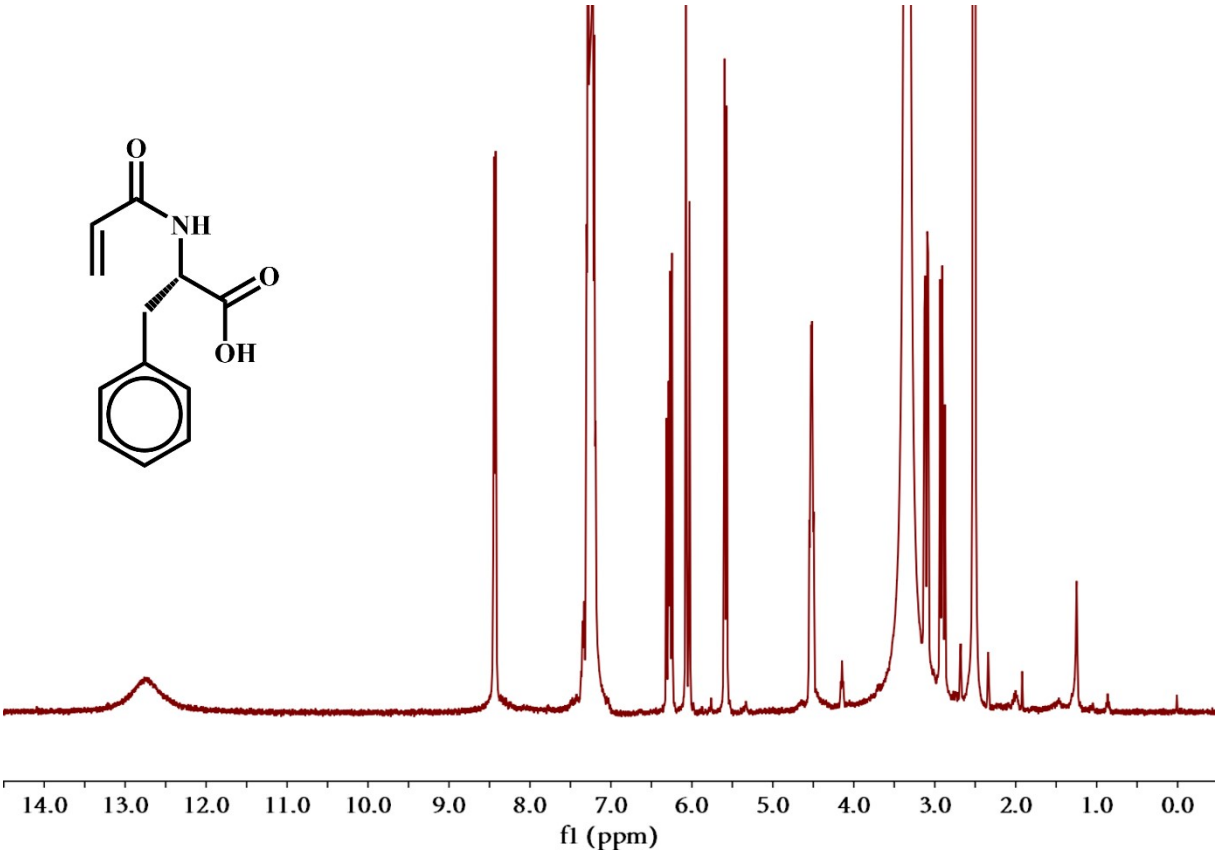

Figure S10. ^{1}H NMR spectrum of Aphe monomer.